Nordic Hydrology, 17, 1986, 93-114

Mixing Effects of Carbonate Dissolving Waters on Chemical and $^{13}C/^{12}C$ Compositions

P. Staniaszek and S. Halas
Institute of Physics, Maria Curie-Sklodowska University
20-031 Lublin, Poland

Seasonal variations in chemistry and $^{13}C/^{12}C$ ratios of total inorganic carbon of carbonate dissolving waters are considered in the frame-work of a simplified approach dealing explicitly with major ionic species. The unidirectional evolution models of Deines *et al.* (1974) are supplemented by taking mixing effects into consideration (Wigley and Plummer 1976). These effects, caused mainly by the redistribution of carbon-bearing species in the mixture, are to a great extent nonlinear and unsymmetric with respect to the fraction of the second solution in a binary mixture. The theoretical considerations are supported by observations of many samples taken during a period from January to May 1977 in SW Lublin Upland.

The parameters PCO_2 and $\delta^{13}C$ of a reservoir lose their primary meaning in the case of mixing of waters but investigation of their changes may help in studying some conditions in the soil. During the period of observation (except March) the estimated values of PCO_2 of a reservoir tended to lie in a narrow range of values from $10^{-1.3}$ to $10^{-1.4}$ atm. In March those values were higher due to the large inflow of CO_2-rich waters into the aquifer. The estimated $\delta^{13}C$ values of a reservoir CO_2 spread from -17 to -27 permil during January to March. In April and May those values focused in a narrow range from -22 to -26 permil. This tendency indicates that waters inflowing in March and April transported isotopically lighter CO_2.

Both HCO_3^- content and $\delta^{13}C$ of total carbon versus pH allowed to search inflows of infiltrating water into particular areas of the aquifer. It has been shown that $\delta^{13}C$ investigations are necessary to notice the admixing of waters in certain cases.

Introduction

Deines et al. (1974) developed simplified models of chemical evolution of carbonate dissolving waters. These authors considered dissolution of calcite and dolomite undergoing in purely open or closed system with respect to carbon dioxide, and illustrated the calculated evolution lines by experimental results obtained on samples taken out in Nittany Valley, Pennsylvania. Although the models developed by Deines *et al.* (1974) quite satisfactorily describe the dissolution of carbonate rocks, their usefulness is limited to one-directional process which rarely occurs in nature. Actually a water present in an aquifer is a mixture of waters, most likely evolved under different conditions, collected during a long period. Therefore, the waters discharged at springs should exhibit some seasonal variations in their chemical and carbon isotope composition around steady-state values.

This paper concerns possible variations in pH, $m\mathrm{HCO}_3^-$ and $^{13}C/^{12}C$ ratio and we illustrate our considerations by presenting the analytic observations of many samples taken during a period from January to May 1977 in SW Lublin Upland, Poland.

Description of Sampling Area

The sampling area is a portion of SW Lublin Upland in which Cretaceous and Tertiary bedrock limestones are overlain by aeolian and solifluctional loess of variable thickness, from 1 to 40 m, of Pleistocene origin or, in valleys, by fluvioglacial sands covered by Holocene valley fill. The sampling points are marked on the map in Fig. 1 and their numeration is further used in the text.

Geologic features of Tertiary rocks of SW Lublin Upland have been described by Bielecka (1967), and that of Cretaceous limestones by Pozarycki (1956). Hydrographic and climatic features have been described in detail by Wilgat (1958, 1968) and Janiec (1973, 1980). The present paper uses some of the detailed information given by those authors and this section describes briefly only the most important hydrogeologic features of the investigated area.

The studied area belongs to a rim synclinore, of NW-SE orientation, which separates two hard plates of NE Europe, i.e. the Black Sea and the Russian, from the rim anticlinorium of West Europe. It must be emphasized, however, that the geological structure of this area is highly differentiated due to the Alpine tectonic activity which is also reflected in the morphology of this area. A geological cross-section across the main watershed reveals several distinguished faults which are accompanied by smaller cracks, oriented perpendiculaly to those shown in Fig. 2. The presence of those latter cracks is reflected in the orientation of rivers and streams, which follow the pattern of cracks.

The sampling points in this study represent springs and wells of the highest productivity. Most of them discharge waters accumulated in Tertiary and Cretace-

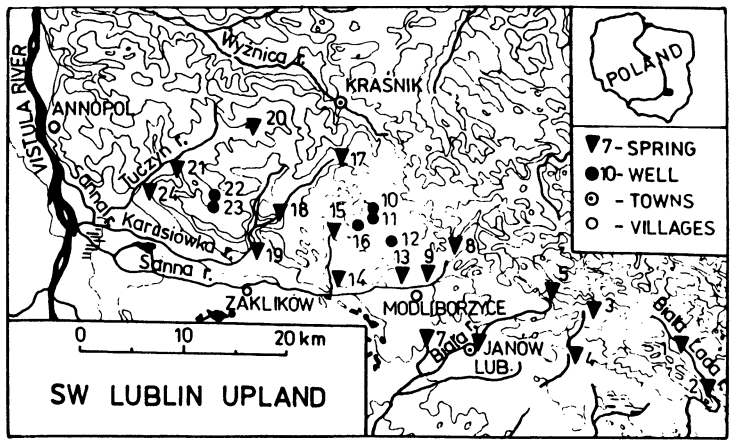

Fig. 1. The sketch map of the study area.

ous limestones. In a few instances, waters from the Jurassic aquifer situated in limestone and/or dolomitic limestone were sampled.

A high and relatively constant productivity of water in SW Lublin Upland, reaching in some instances the rate of over 100 litres per second, is related to the high permeability of limestone rock, especially in Cretaceous formation which has a dense net of fissions of the diaclasial type. Another factor increasing the productivity of water in this area is the presence of Sarmatian clay formation (Kracowiec clays) in the surrounding of the three-fault threshold (see Fig. 2) which isolates the

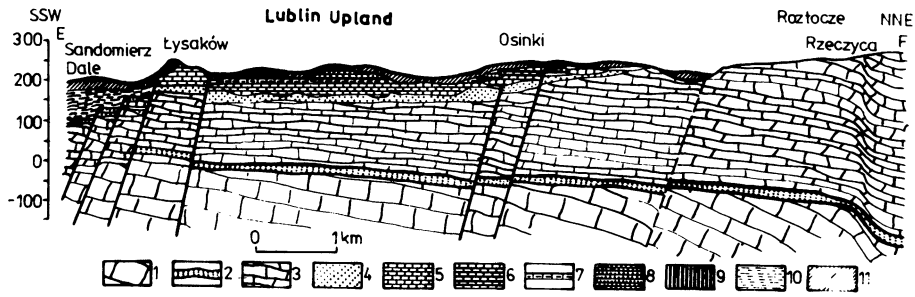

Fig. 2. Section through the margin of the Lublin Upland near Lysakow. Jurassic 1. marls, limestones and dolomites. Cretaceous 2. pale-green sands (Albian, Cenomanian) 3. opokas and limestone (Turonian, Emscherian, Santonian) Tertiary 4. white and pale-green sands (Tortonian-sub-Lithothamnian horizon) 5. finely lithothamnian detritic limestone (Tortonian-Lithothamnian horizon) 6. reef limestone with "Haliotis" 7. marls with "Chlamys scissa" along with Ervilia bed at the top (Tortonian-supra-Lithothamnian horizon) 8. detritic limestone sands and sandstones (Tortonian + Sarmatian) 9. serpulian reef limestone (Sarmatian) 10. Krakowiec clays (Sarmatian) Quaternary 11. loesses, boulder clays and sands.

Table 1 – General data as to the sampling points arranged according to the code numbers as in Fig. 1.

Code No.	Location[a]	Aquifer[b]	$\delta^{13}C$ of bedrock carbonate[c]	Drainage -basin	
1	Goraj, ss	soft ls, C		Biala Lada	Bukowa river basin
2	Abramow, ss	soft ls, C		Biala Lada	
3	Branew, ss	reef ls, T	−1.78	Branew	
4	Krzemien, s	reef-detrial ls, T	+2.60	Branew	
5	Godziszow I, s	reef-detrial ls, T		Biala	
6	Janow Lub., ss	detrial ls, T	−0.58	Biala	
7	Borownica	detrial-reef ls, T		Borownica	
8	Wierzchowiska I, ss	soft ls, C		Sanna	Sanna river basin
9	Lute, s	soft detrial ls, T	+0.03	Lutynka	
10	Kol. Polichna G., w	ls, C		Lutynka	
11	Huta Jozefow, w	ls, C		Stanianka	
12	Zarajec	detrial ls, T+ls, C	+1.95	Lutynka	
13	Dabie, ss	detrial ls, T	−0.08	Lutynka	
14	Potoczek, s	detrial ls, T	−0.24	Stanianka	
15	Potok Stany	marly ls, C	+1.99	Stanianka	
16	Kol. Stany III, w	marly ls, C		Stanianka	
17	Rzeczyca Ksieza, ss	ls, C	+1.98	Karasiowka	
18	Lychow, ss	ls, C	+1.60	Karasiowka	
19	Zdiechowice, s	detrial-reef ls, T	−0.76	Karasiowka	
20	Olbiecin, s	ls, C	+2.14	Tuczyn	
21	Goscierardow, s	sands, Q		Tuczyn	
22	Salomin Dlugosz, w	dolomitic ls, J	+2.34	Tuczyn	
23	Salomin Skrzypek, w	sands, J		Tuczyn	
24	Mniszek-Lany, ss	ls, C		Tuczyn	

[a]here s = spring, ss = springs, w = well

[b]here ls = limestone, J = Jurassic, C = Cretaceous, T = Tertiary, Quaternary

[c] in per mil PDB, data taken from Halas et al. (1979).

uplifted aquifers. The most productive water discharges are located along the above mentioned tectonic lines. Highly productive artesian and sub-artesian wells occur in some places, below that threshold (Janow Lubelski, Zaklikow, Frampol, Bilgoraj). Long-term observations of the temperature of underground waters in the described area (Janiec 1980) reveal small seasonal variations ranging from 9.0 to 9.6°C. Some other data on the sampling points are summarized in Table 1.

Analytical Procedures

One-litre bottles were filled with water samples collected for measuring pH and specific conductance (μ) and immediately transported to the laboratory. The pH and μ measurements were performed within several hours after sampling. By transporting several bottles of tap water into the field and back to the laboratory, it has been proved that the pH of carbonate water remains almost constant during the first three hours after sampling.

Total dissolved carbon was precipitated as $BaCO_3$ in the field using one-litre glass bottles filled with 75 ml of saturated $BaCl_2$-NH_4OH solution. The precipitate was carefully removed from the bottle using ultrasonic bath, then rinsed by boiled bidistillate water, centrifuged and finally dried at 75°C for several days. $BaCO_3$ obtained in this way was weighted and $mHCO_3^-$ was calculated from the pH and total mass of the precipitate. CO_2 was subsequently derived for isotope analysis of carbon total from $BaCO_3$ by means of 100 %-H_3PO_4 in a vacuum line (McCrea 1950). The isotope ratio determination was carried out by means of a standard Nier-type spectrometer with an improved inlet system (Halas 1979) and on-line data processing (Halas and Skorzynski 1980, 1981).

The Solenhofen Limestone (NBS-20) was used for the calibration of the working standard. The precision of 0.05 permil was obtained in $\delta^{13}C$ and $\delta^{18}O$ measurements, and 0.05 in pH and about 2 percent in $mHCO_3^-$ determinations. The $\delta^{18}O$ values were determined occasionally in order to introduce the correction factor in $\delta^{13}C$ (Craig 1957).

Medium System Conditions Model

Holland et al. (1964), Thrailkill (1968) and Langmuir (1971) discussed open and closed system models for the solution of carbonate rocks. Deines *et al.* (1974) demonstrated simple models of the dissolution of calcite and dolomite rocks. Of course, more sophisticated and complicated models for the chemistry of water in a hydrologic system have been developed since 1974 (Plummer *et al.* 1975, 1976, Plummer 1977, Wigley *et al.* 1978, 1979, Plummer and Back 1980, Plummer *et al.* 1983). The models of Deines *et al.* (1974), however, still seem to be reliable and suitable for the interpretation of actual field data, regarding the chemistry and $^{13}C/^{12}C$ ratios of total inorganic carbon dissolved, if the mixing of two carbonate waters is taken into account. Some of the springs and wells investigated are located on loessal terrains. Since loesses contain carbonates which may react with CO_2 dissolved in water, we introduce the medium system conditions model (MSC) which takes soil carbonate dissolution into account.

The dissolution of the soil carbonates occurs under open system conditions (OSC), i.e. in the presence of the large and homogeneous reservoir of a gas phase of CO_2 with constant pressure (PCO_2) which will be denoted as PCO_{2RES}. A

continuous exchange of carbon isotopes is assumed between the reservoir CO_2 and the solution, because this exchange proceeds relatively fast, within a few hours (Szaran and Zuk 1980). When the water infiltrates into the carbonate rocks, it is isolated from the reservoir CO_2 and the dissolution of carbonates is continued under the closed system conditions (CSC). We introduce a parameter α as a ratio

$$\alpha = \frac{mCa_B^{2+}}{mCa_T^{2+}} \tag{1}$$

where mCa_B^{2+} is a molality of calcium which was introduced into the water under OSC (this value is attained at point B in Fig. 3a), mCa_T^{2+} is the total molality of calcium which was introduced into the water during carbonate dissolution up to the saturation point T (Fig. 3a). Saturation with calcite is attained when the calcite saturation index (SIc) is equal to zero.

Molality of H_2CO_3 up to the border point B is constant and it is determined by Henry's law

$$mH_2CO_{3i} = mH_2CO_{3B} = KCO_2\, PCO_{2RES} \tag{2}$$

where KCO_2 is equilibrium constant, index i denotes the initial point at which the dissolution started, PCO_{2RES} is an assumed parameter. Molality of H_2CO_3 under CSC is expressed by the formula

$$mH_2CO_3 = mH_2CO_{3B} - (mCa^{2+} - mCa_B^{2+}) \tag{3}$$

where molality of Ca^{2+} is given by

$$mCa^{2+} = \frac{mHCO_3^- - mHCO_{3i}^-}{2} \tag{4}$$

where $mHCO_{3i}^-$ is calculated for the assumed pH_i as outlined below.

From Eqs. (2)-(4) and the equilibrium equation, which involves the first dissociation constant of CO_2

$$K_1 = \frac{aH^+\, \gamma HCO_3^-\, mHCO_3^-}{mH_2CO_3} \tag{5}$$

one obtains the formula for molality of HCO_3^- as a function of activity of hydrogen ions,

$$mHCO_3^- = \frac{KCO_2\, PCO_{2RES} + \frac{1}{2}\, mHCO_{3i} + mCa_B^{2+}}{\frac{1}{2} + aH^+\, \gamma HCO_3^- / K_1} \tag{6}$$

Using the equilibrium equation which involves the second dissociation constant K_2, one obtains the following expression for the molality of CO_3^{2-}

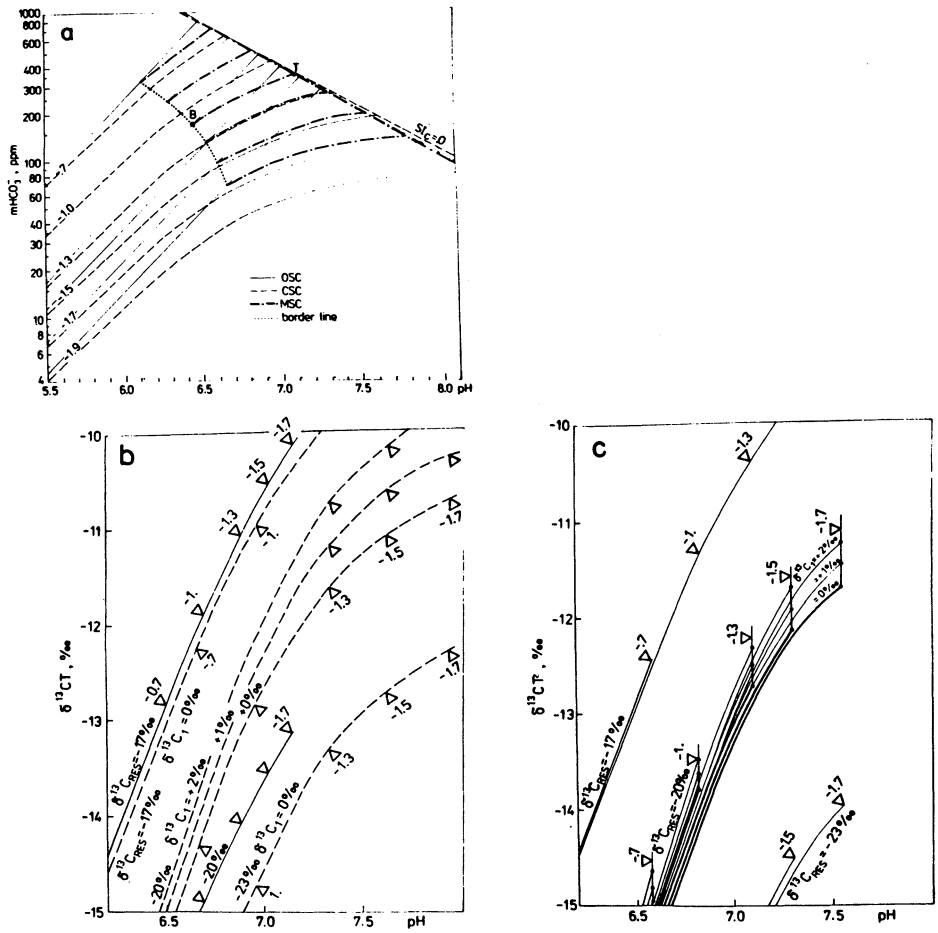

Fig. 3. a) Plots of $m\mathrm{HCO}_3^-$ value versus pH calculated for OSC, MSC and CSC models.
b) Plots of $\delta^{13}CT$ versus pH for CSC (dashed line) and OSC (bold line). Triangles point to the saturation states, at which the curves terminate, for log (PCO_{2RES}) is specified along some of the curves.
c) Plots of $\delta^{13}CT$ versus pH for MSC. Main lines were drawn for $\delta^{13}C_1 = 0‰$ (see explanation in the text).

$$m\mathrm{CO}_3^{2-} = \frac{K_2\, m\mathrm{HCO}_3^-\, \gamma\mathrm{HCO}_3^-}{a\mathrm{H}^+\, \gamma\mathrm{CO}_3^{2-}} \qquad (7)$$

where $\gamma\mathrm{HCO}_3^-$ and $\gamma\mathrm{CO}_3^{2-}$ are activity coefficients of these species.

In order to complete the calculation of the ionic strength one must estimate $m\mathrm{OH}^-$ from the dissociation equation of water

$$K_w = a\mathrm{H}^+\, a\mathrm{OH}^- \qquad (8)$$

In calculation of the molalities of the considered species we used the following iterative procedure. γ-values are assumed to be equal to one at the first step, then molalities and ionic strength are estimated from the complete Debye-Hückel expression (c.f. Truesdell and Jones 1974; Plummer and Busenberg 1982). The parameter $m\mathrm{HCO}_{3i}^{-}$ is calculated iteratively from Eq. (6) for a given pH_i assuming a realistic value at the first step. Constant Kw was taken from Ackermann (1958). Constants $K\mathrm{CO}_2$, K_1 and K_2 were taken from Plummer and Busenberg (1982).

The isostopic composition of carbon total

$$CT = m\mathrm{H}_2\mathrm{CO}_3 + m\mathrm{HCO}_3^{-} + m\mathrm{CO}_3^{2-} \tag{9}$$

we obtain from the formula

$$\delta^{13}CT \equiv (m\mathrm{H}_2\mathrm{CO}_{3i}\,\delta^{13}\mathrm{C}_{\mathrm{H}_2\mathrm{CO}_3} + m\mathrm{HCO}_3^{-}\,\delta^{13}\mathrm{C}_{\mathrm{HCO}_3^-} + m\mathrm{CO}_3^{2-}\,\delta^{13}\mathrm{C}_{\mathrm{CO}_3^{2-}} + (m\mathrm{Ca}^{2+} - m\mathrm{Ca}_B^{2+})\,\delta^{13}\mathrm{C}_1) / CT \tag{10}$$

where $\delta^{13}\mathrm{C}_1$ is isotopic composition of carbonate rocks being dissolved under CSC.

Results of calculation for $\alpha = 0.5$ and $\mathrm{pH}_i = 5.0$ are shown in fig. 3a, b, c. We may compare the closed, open and medium system models by the graphs $m\mathrm{HCO}_3^{-}$ versus pH in Fig. 3a and by the graphs $\delta^{13}CT$ versus pH in Figs. 3b, c. The closed system evolution lines along with those for the open system are shown in Fig. 3b. The curve for $\delta^{13}\mathrm{C}_{\mathrm{RES}} = -20‰$ in the closed model is splitted in three path: for $\delta^{13}\mathrm{C}_1 = 0$, +1 and +2 permil. Since the change of $P\mathrm{CO}_{2\mathrm{RES}}$ from $10^{-1.0}$ to $10^{-1.7}$ yields the difference in $\delta^{13}CT$ of about 0.1‰, we neglected this to avoid complication of the figure. Some paths for MSC model are shown in Fig. 3c. In this case the difference in $\delta^{13}CT$ for $P\mathrm{CO}_{2\mathrm{RES}} = 10^{-1.0}$ to $10^{-1.7}$ atm is variable and it depends on $\delta^{13}\mathrm{C}_{\mathrm{RES}}$. This difference was about 0.38‰ for $\delta^{13}\mathrm{C}_{\mathrm{RES}} = -20‰$ and 0.08‰ for $\delta^{13}\mathrm{C}_{\mathrm{RES}} = -17‰$ (Fig. 3c). The line for $\delta^{13}\mathrm{C}_{\mathrm{RES}} = -20‰$ is split for $\delta^{13}\mathrm{C}_1 = 0$, +1 and +2 permil.

Initial pH value is considered as parameter in the presented models. This value depends on many conditions. For example it depends on air pollution by sulfur dioxide and/or nitric oxides. However, the sensitivity of models considered, on pH_i is rather small, as is shown below.

Acid rains causes increase of amounts of ions which are neglected in presented models. Janiec (1980) performed occasionally total chemical analysis of investigated waters. From his investigation the ratio of HCO_3^{-} (in mval/l) to all anions (in mval/l) is from 72 to 96 % and the ratio of Ca^{2+} (in mval/l) to all cations (in mval/l) is from 73 to 100 % with one exception, spring No. 17, which had the last ratio about 59 % in May. Most springs and wells have contribution of HCO_3^{-} more than 90 % and contribution of Ca^{2+} more than 80 %. In such a case we may neglect all minor species. The comparison of values computed in this way with those determined from total analyses, of those waters, shows differences only a few per cent, or less between them.

Mixing Effects

An aquifer contains waters from many inflows collected, mixed and discharged for years and these waters have some average values of PCO_2 and $\delta^{13}CT$. When a new water flows into the aquifer, these values are changed. These changes depend not only on the amount of the water added in proportion to the amount of water in the aquifer but also on how far the parameters of the new water differ from those of the aquifer water. Mixing of carbonate waters have been considered by Wigley and Plummer (1976) on the basis of particular form of the charge balance equation to avoid having to balance H^+ which is computationally inefficient. In that paper H^+ is calculated indirectly from total alkalinity and total carbon. The authors presented the nonlinear behaviour of calcite saturation index (SIc) and pH value of a binary mixture with respect to the fraction of the component being admixed.

In our simplified approach the chemical compositions of waters to be mixed are calculated by using models of Deines *et al.* (1974). As a consequence of using those models we get electrically unbalanced solutions though their major species are quite precisely determined. The obvious difficulties which arise with this "artificial" electric charge in the chemistry calculation of a mixture may be avoided by applying the charge conservation equation to this apparent charge, the specific value of which (in coulombs/kg) is proportional to

$$R \equiv 2\,mCa^{2+} + mH^{+} - (2\,mCO_3^{2-} + mHCO_3^{-} + mOH^{-}) \qquad (11)$$

Let R_1 and R_2 denote the specific charge of the solutions being mixed. Thus the R of the mixture may be expressed as a linear combination of R-values of the end-members

$$R = x\,R_1 + (1-x)\,R_2 \qquad (12)$$

where x is the fraction of solution 1 in the mixture.

The conservation principle provides three further equations of similar character

$$CT \equiv x\,CT_1 + (1-x)\,CT_2 \qquad (13)$$

$$mCa^{2+} = x\,m_1Ca^{2+} + (1-x)\,m_2Ca^{2+} \qquad (14)$$

$$\delta^{13}CT \equiv x\,\delta_1^{13}CT + (1-x)\,\delta_2^{13}CT \qquad (15)$$

where CT denotes carbon total in a solution, see Eq. (9).

The calculation of the chemical composition of a mixture starts from an evaluation of the activity of hydrogen ions aH^+. For this goal the expressions for CT and R values of the mixture are rewritten using respective equilibrium constants as follows

$$CT \equiv mHCO_3^{-}\left(1 + \frac{mH_2CO_3}{mHCO_3^{-}} + \frac{mCO_3^{2-}}{mHCO_3^{-}}\right) = mHCO_3^{-}\left(1 + \frac{\gamma HCO_3^{-}\,aH^{+}}{K_1} + \frac{\gamma HCO_3^{-}K_2}{\gamma CO_3^{2-}\,aH^{+}}\right) \qquad (16)$$

$$R = 2m\mathrm{Ca}^{2+} + \frac{a\mathrm{H}^+}{\gamma\mathrm{H}^+} - m\mathrm{HCO}_3^- \left(1 + \frac{2\gamma\mathrm{HCO}_3^- K}{\gamma\mathrm{CO}_3^{2-}\ \mathrm{H}^+}\right) - \frac{K_w}{\gamma\mathrm{OH}^- a\mathrm{H}^+} \qquad (17)$$

By eliminating $m\mathrm{HCO}_3^-$ from the above equations, one obtains the following equation for $y = a\mathrm{H}^+$

$$y^4 + Ay^3 + By^2 + Cy + D = 0 \qquad (18)$$

where

$$A = K_1 / \gamma\mathrm{HCO}_3^- + (2m\mathrm{Ca}^{2+} - R)\gamma\mathrm{HCO}_3^- \quad , \ \gamma\mathrm{H}^+ \approx \gamma\mathrm{OH}^- \approx \gamma\mathrm{HCO}_3^-$$

$$B = K_1 (2m\mathrm{Ca}^{2+} - R + K_2 / \gamma\mathrm{CO}_3^{2-} - CT) - K_w$$

$$C = K_1 (\gamma\mathrm{HCO}_3^- K_2 (2m\mathrm{Ca}^{2+} - R - 2CT) / \gamma\mathrm{CO}_3^{2-} - K_w / \gamma\mathrm{HCO}_3^-)$$

$$D \equiv K_1 K_2 K_w / \gamma\mathrm{CO}_3^{2-}$$

The appropriate real root of this polynomical can be computed by the Newton method using the weighted average of pH-values in the first step of the calculation. Actually further simplifications are justified when the calculation is limited to the pH ranging from 5 to 8. In this range of pH values, for a typical carbonate water ($2m\mathrm{Ca}^{2+} \approx m\mathrm{HCO}_3^- \approx 0.01$ moles/kg), term D Eq. (18) and some contributions of A, B, and C coefficients may be safely neglected.

Thus a considerably simplified equation

$$y^3 + ((2m\mathrm{Ca}^{2+} - R)\gamma\mathrm{HCO}_3^- + K_1 / \gamma\mathrm{HCO}_3^-) y^2 + K_1 (2m\mathrm{Ca}^{2+} - R - CT) y + K_1 K_2 \gamma\mathrm{HCO}_3^- (2m\mathrm{Ca}^{2+} - R - 2CT) / \gamma\mathrm{CO}_3^{2-} \equiv 0 \qquad (19)$$

is to be solved. The last term in Eq. (19) remains significant only if pH approaches 8.0.

Once $a\mathrm{H}^+$ is evaluated the $m\mathrm{HCO}_3^-$ of the mixture is calculated from Eqs. (13) and (16) while $m\mathrm{CO}_3^{2-}$ is calculated from Eq. (7).

The molalities of the major species in the mixture are calculated iteratively as described in the previous section.

The chemical characteristics of the model waters to be mixed are presented in Table 2. A wide differentiation in chemical composition of those waters allows to search for the changes in water chemistry during mixing. It is assumed that all the waters considered evolved under CSC conditions.

Fig. 4 shows the combined mixing curves for $m\mathrm{HCO}_3^-$ vs pH with x values marked along the curves. These curves have been plotted on the background of the selected carbonate-water evolution lines. Let us consider the following two extreme cases of closed-system mixing.

Table 2 – The chemical composition of model solutions* used in mixing calculations. The molalities of HCO_3^-, and Ca^{2+} are expressed in ppm, while the ionic strength, $I = (mHCO_3^- + mH^+ + mOH^- + 4(mCO_3^{2-} + mCa^{2+}))$ /2 was calculated by substituting the molalities in mmoles per 1000 g of the solution. The partial pressure of CO_2 for waters was calculated from expression: $PCO_2 = mH_2CO_3/KCO_2$.

No.	$-\log(\frac{PCO_{2RES}}{atm})$	$-\log(\frac{PCO_2}{atm})$	ppm pH	ppm HCO_3^-	Ca^{2+}	I	SI
1	0.7	0.97	6.67	645	204	0.0155	0
2	1.0	1.43	6.97	432	138	0.0104	0
3	1.3	1.99	7.33	272	88	0.0066	0
4	1.5	2.42	7.61	190	61	0.0046	0
5	1.7	2.91	7.94	128	41	0.0031	0
6	1.0	1.20	6.50	250	78	0.0060	−1.02
7	1.3	1.57	6.70	162	51	0.0039	−1.14
8	1.0	1.10	6.20	151	46	0.0035	−1.71
9	1.5	1.63	6.20	47	14	0.0011	−2.63

* Computed according to the models developed by Deines et al. (1974) assuming the initial pH value before carbonate dissolution $pH_i = 5.0$ for each water.

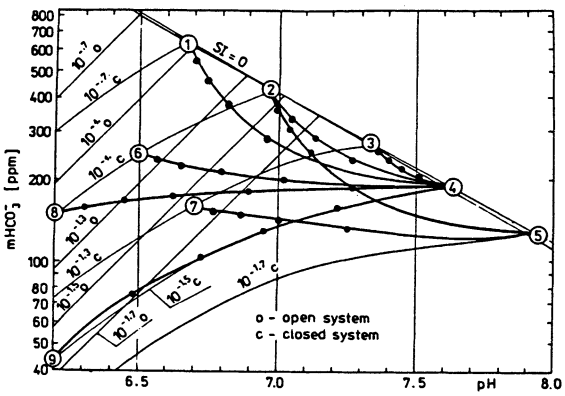

Fig. 4. Combined plots $mHCO_3^-$ versus pH for mixtures of two waters (from Table 2) plotted along the lines of calcium carbonate dissolution model of Deines *et al.* (1974). The mixing curves joining initial compositions of two waters are marked by dots for every .2 change in x-value.

1) A saturated water ($SI = 0$) is admixed with other saturated water which has a higher PCO_2 or undersaturated one evolving under a higher PCO_2.
2) A highly undersaturated water is admixed with a small fraction of a saturated water which evolved under the same PCO_2.

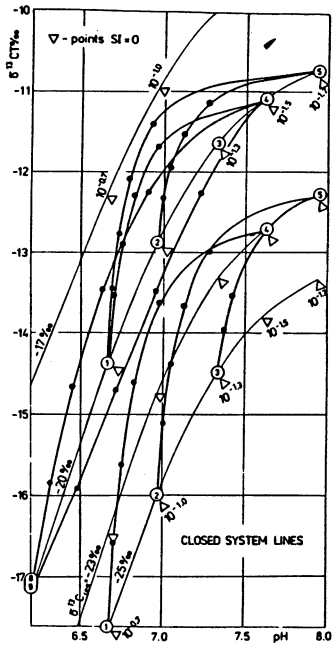

Fig. 5.
Combined plots $\delta^{13}CT$ of the mixture versus pH on the background of the CSC model evolution lines (Deines *et al.* 1974). The mixing curves joining initial compositions of two waters are marked by dots for every .2 change in *x*-value. The initial pH values are taken from Table 2, while $\delta^{13}CT$ were calculated assuming $\delta^{13}C_{RES} = -20$, -23 and -25‰. Triangles show points of $SI \equiv 0$ on the evolution lines for PCO_2 specified.

In the first case, since pH is highly sensitive to the mixing process, an admixing can be easily recognized, while in the second case a point representing pH and $mHCO_3^-$ of the water to be examined will move along a closed system evolution line (e.g. water 9 admixed with water 4, Fig. 4). Thus mixing will be difficult to recognize from pH and HCO_3^- data. The second case, however, is less likely in natural conditions. We shall see that the use of $\delta^{13}CT$ in such a case may allow to distinguish between carbonate dissolution and the mixing process.

Fig. 5 shows the combined mixing curves for $\delta^{13}CT$ vs pH along with some selected carbonate-water evolution lines calculated according to the simplified model of Deines *et al.* (1974). The parameter *x* varies along the mixing curves, and it is marked for every 0.2 change in the fractional composition of the mixture. While comparing the mixing curves with those describing the evolution of a single water under certain conditions (CSC, different $\delta^{13}C_{RES}$) it is clear that the mixing effects can drastically change both pH and $\delta^{13}CT$ due to the admixture of a small fraction of water different from that accumulated in the aquifer. Thus $\delta^{13}C_{RES}$ derived under the assumption of no mixing by backtracking along a closed system path may be substantially in error.

If the aquifer water was saturated at low PCO_2 and subsequently admixed with a water saturated (or undersaturated) at a higher PCO_2, but at the same $\delta^{13}C_{RES}$, then a major change in $\delta^{13}CT$ and pH will occur. Such a case is shown in Fig. 5, pairs 4-1, 4-8 and 4-9. A more significant change will take place when the water to be admixed differs in $\delta^{13}C_{RES}$ (consider mixing line 4-1 joining lines $\delta^{13}C_{RES} = -23$

and −25 permil, for example).

In a reverse situation, i.e. when a small fraction of low PCO_2 water is admixed with a CO_2-rich water, one can predominantly distinguish between carbonate dissolution and the mixing process. Let us consider, for example, the mixing lines 1-4 in Fig. 5. The line which starts and terminates on the evolution line for $\delta^{13}C_{RES}$ = −20‰ deviates from this line in a similar way as that joining the evolution lines for $\delta^{13}C_{RES}$ = −25 and −23 permil. In rather rare cases, however, the change in pH and $\delta^{13}CT$ can tend along the evolution line. Such a situation is anticipated, for example, in case of water, the chemistry of which is somewhere between that of waters 8 and 9. It should be noted that the mixing curve lies below the evolution line when the algebraic effect exceeds the PCO_2 effect (Wigley and Plummer 1976). Therefore, if these effects compensate each other, then the changes in pH and $\delta^{13}CT$ will move along the evolution line and, thus, the mixing process cannot be distinguished from the carbonate dissolution.

The situation when both processes may be indistinguishable may occur rather seldom because natural variation of $\delta^{13}C_{RES}$ diminishes the probability that the mixed waters evolved under identical $\delta^{13}C_{RES}$. Thus the mixing process may be frequently recognized from $\delta^{13}CT$ and pH though $m\text{HCO}_3^-$ and pH data are insufficient for this purpose. More about model presented above in Staniaszek and Halas (1985).

Results and Discussion

The period of our observation was very advantageous for studies of infiltration rate since numerous inflow events were feeding the limestone aquifer in late autumn, winter and early spring, whereas the feeding stopped in April by an increased evaporation of rain water and by an increase of biological activity in the soil. The appropriate meteorological data are shown in Fig. 6.

Results of the investigation are shown in Table 3 and Figs. 7, 8, 9, where we assumed for the model lines that pH_i value of the soil water was 5.0. This is in agreement with the soil studies performed at our University (Uziak *et al.* 1980/1981). Actually the change of pH_i from 4 to 6, yields such a small difference in the shape of the curves in Figs. 3, that it may be neglected in this consideration. The difference in $m\text{HCO}_3^-$ is about 40 mg/l and in $\delta^{13}CT$ is about 0.1‰, when pH_i changes from 5 to 6.

To fit theoretical CSC curves to the experimental data the following isotopic composition of the rocks $\delta^{13}C_1$ were assumed: −0.2, +2.0, +2.2 permil for Tertiary, Cretaceous and Jurassic limestones, respectively. These values are averages of some rock samples taken from the study area (Halas *et al.* 1979).

In Fig. 8 seasonal variations in the $\delta^{13}CT$ versus pH are shown, whilst in Fig. 9 the $m\text{HCO}_3^-$ versus pH. From these figures we may draw the conclusion that these

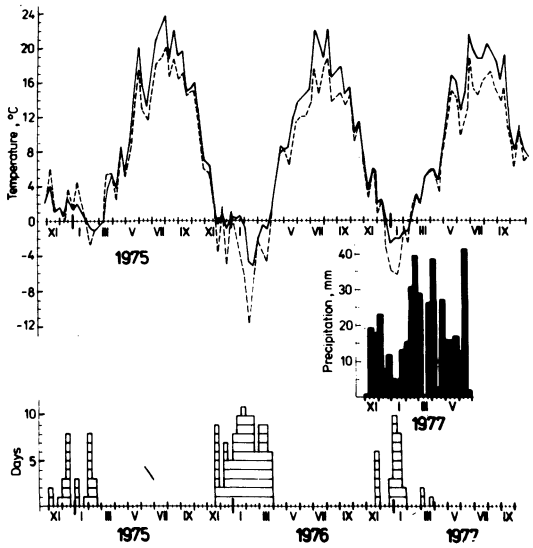

Fig. 6.
Meteorological data. Daily temperatures of the air (border line) and the soil 5 cm under the surface (dashed line). In addition there are total decade precipitations and the number of days with snow lying on the surface are shown.

waters were saturated under CSC or MSC. The carbonate contents in loess in the study area is lower than in other areas of Lublin Upland and because of that, it may be neglected in our consideration (Klimowicz Z. – personal commun.). The parameter α in this case is nearly zero. For this reason CSC theoretical curves were fitted to the experimental data. The obtained values of PCO_{2RES} and $\delta^{13}C_{RES}$ are collected in Fig. 7. The estimated values of $\delta^{13}C_{RES}$ are consistent with $\delta^{13}C$ of the soil CO_2 studied by Reardon *et al.* (1979).

It should be mentioned, however, that the curves drawn according to Deines *et al.* (1974), do not indicate the real, average values of PCO_{2RES} and $\delta^{13}C_{RES}$, but some modified values only. The modifications are mainly caused by the mixing process described above. Inasmuch as a small inflow of water with PCO_2 slightly higher may change pH significantly, the theoretical curves fitted to the observed data yield $\delta^{13}C_{RES}$ too high, despite of the fact that the inflowing water may evolve under identical $\delta^{13}C_{RES}$ as that accumulated in the aquifer. This difference may be as high as +3‰ when two waters differing in PCO_2 by about 0.1 atm have been mixed (see Fig. 5). By investigation of changes of parameters PCO_{2RES} and $\delta^{13}C_{RES}$ we may notice only some trends but nothing can be said about the exact values of $\delta^{13}C$ and PCO_2 in the soil, even if we know what kind of model is the most reliable.

The histograms for PCO_{2RES}, indicate that in January most waters evolved under PCO_{2RES} from $10^{-1.3}$ to $10^{-1.4}$ atm or less. In February significant inflows of water of higher PCO_2 into aquifers took place, thus most of the waters sampled in March show PCO_{2RES} higher than $10^{-1.3}$ atm. In April and May the number of samples with PCO_{2RES} from $10^{-1.3}$ to $10^{-1.4}$ atm, or close to this range, increased. This indicates the inflow of waters with PCO_2 lower than that in March. An alternative explanation of this shift in histograms may be a small loss of CO_2 from

Table 3 – Chemical and carbon isotope compositon of the spring and well waters analyzed in this study. Molality of HCO_3^- is in ppm, $\delta^{13}CT$ in permil vs PDB and specific conductance (μ) in $10^{-6}\Omega^{-1}cm^{-1}$.

	9 and 18-21 1-8 and 10-17		31.I.1977 20.I.1977		3.III.1977 16.III.1977				1.IV.1977				5.V.1977			
No.	pH	HCO_3^-	$\delta^{13}CT$	μ	pH	HCO_3^-	$\delta^{13}CT$	μ	pH	HCO_3^-	$\delta^{13}CT$	μ	pH	HCO_3^-	$\delta^{13}CT$	μ
1	2	3	4	5	6	7	8	9	10	11	12	13	14	15	16	17
1	6.4	169	−14.34	529.74	6.5	217	−14.07	986.00	7.3	368	−14.12	500.58	7.6	382	−13.87	558.90
2	7.1	300	−14.47	500.58	6.75	260	−14.44	461.70	7.0	287	−14.92	483.57	7.5	355	−13.60	520.02
3	6.9	168	−14.32	493.29	6.8	304	−13.56	461.70	6.9	269	−14.10	456.84	7.6	349	−13.30	505.44
4	7.0	136	−12.68	340.20	7.0	162	−13.11	294.03	7.25	197	−13.37	312.50	7.7	207	−12.06	364.50
5	7.0	210	−13.90	432.54	6.9	225	−14.25	391.23	7.1	202	−13.94	408.24	7.6	230	−13.25	461.70
6	6.8	132	−12.96	408.24	7.4	206	−14.10	320.76	7.3	220	−13.57	359.64	7.7	257	−12.59	403.38
7	7.0	134	−12.74	369.36	6.5	131	−13.53	291.60	7.4	101	−13.20	329.51	7.8	186	−12.09	369.36
8	7.1	283	−13.14	534.60	6.3	173	−13.98	500.58	6.8	285	−14.08	500.58	7.45	397	−13.42	568.62
9	7.1	186	−13.45	369.36	7.1	169	−13.27	325.62	7.3	217	−13.86	364.50	7.65	255	−12.70	717.96
10	7.6	123	−13.26	208.98	6.9	127	−13.97	251.70	7.4	141	−13.62	278.48	7.80	181	−12.89	320.76
11	8.0	179	– 4.95*	510.30	6.6	292	−15.15	753.30	7.3	375	−13.44	729.00	7.8	408	−12.75	860.22
12	6.9	162	−12.75	478.70	6.65	190	−14.50	500.60	6.95	256	−14.38	500.58	7.85	300	−12.64	583.20
13	6.9	184	−13.22	408.24	7.30	239	−13.12	354.78	7.00	217	−13.60	379.08	7.65	281	−12.42	417.96
14	6.4	94	−13.37	376.65	6.60	134	−13.26	296.46	7.1	222	−13.50	337.77	7.85	214	−12.43	379.08
15	6.9	205	−13.71	425.25	6.40	192	−13.34	388.80	7.2	264	−14.18	413.10	7.45	289	−12.62	476.28
16	7.0	213	−13.45	456.84	6.75	177	−12.32	357.70	7.4	265	−12.88	357.21	7.5	272	−13.44	408.24
17	7.0	198	−14.51	420.39	7.25	248	−14.16	383.94	7.13	250	−13.30	403.38	7.5	272	−13.44	456.84
18	6.8	162	−12.86	381.51	7.3	243	−13.26	335.34	7.2	233	−14.07	363.09	7.7	276	−11.84	408.24
19	7.3	190	−12.33	340.20	7.05	181	−12.91	318.33	7.0	218	−13.78	349.43	7.75	249	−12.58	398.52
20	7.7	278	−13.57	458.30	6.85	243	−14.03	423.30	6.9	270	−14.41	937.90	7.55	306	−13.08	486.00
21	7.4	220	−11.16	379.08	7.3	234	−12.03	366.93	7.2	260	−11.94	394.15	7.8	270	−11.44	447.12
22	6.6	291	−12.05	772.74	7.2	366	−11.80	777.60	6.8	382	−13.32	777.60	7.4	552	−12.77	874.80
23	7.2	208	−11.35	811.62	7.75	279	−11.50	826.20	7.3	243	−12.23	821.34	8.0	295	−10.90	923.40
24	7.2	206	−12.02	391.23	7.4	256	−12.32	383.94	7.2	236	−12.72	393.66	7.65	362	−12.30	432.54

* This value was treated as outliner.

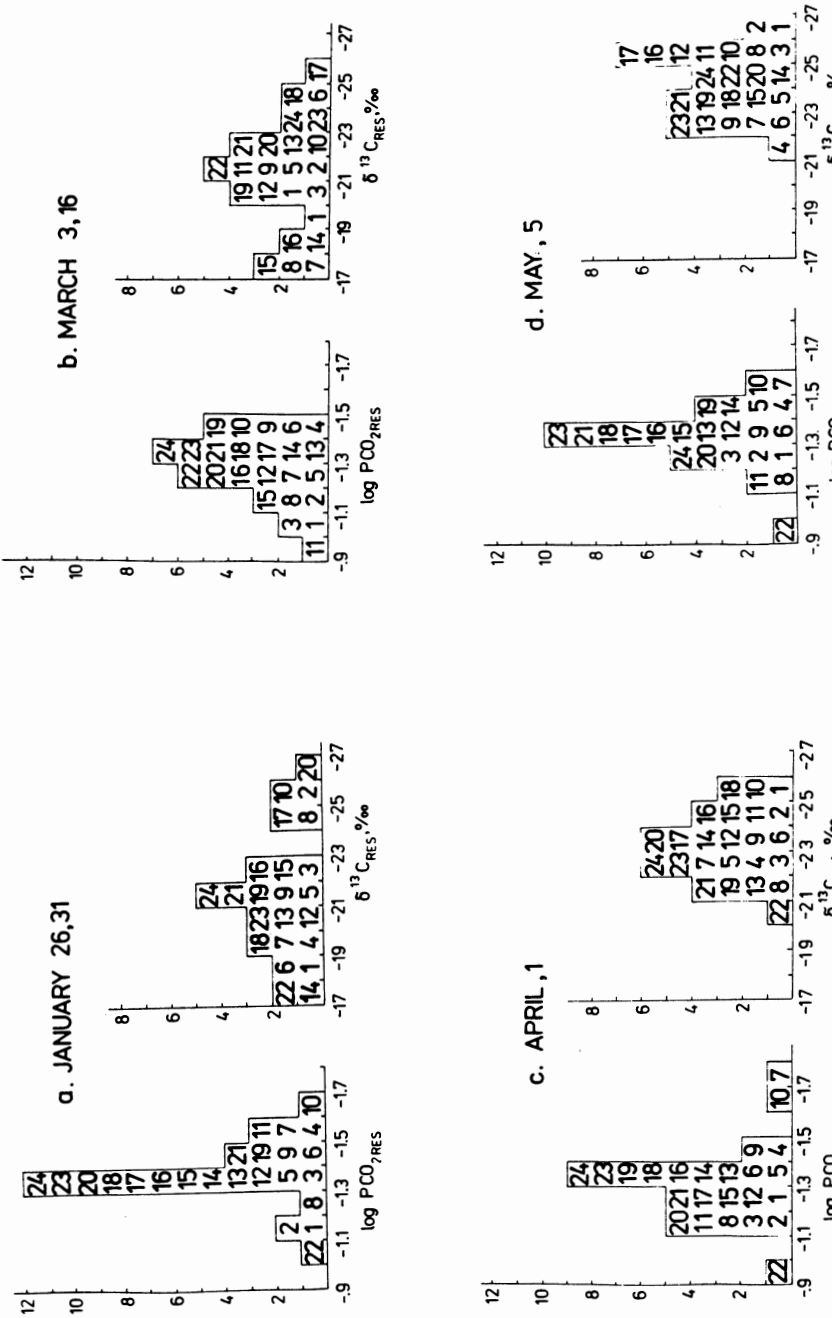

Fig. 7. Histograms for PCO_{2RES} and $d^{13}C_{RES}$ obtained by fitting theoretical paths to the experimental data (see text). The numbers denote springs and wells.

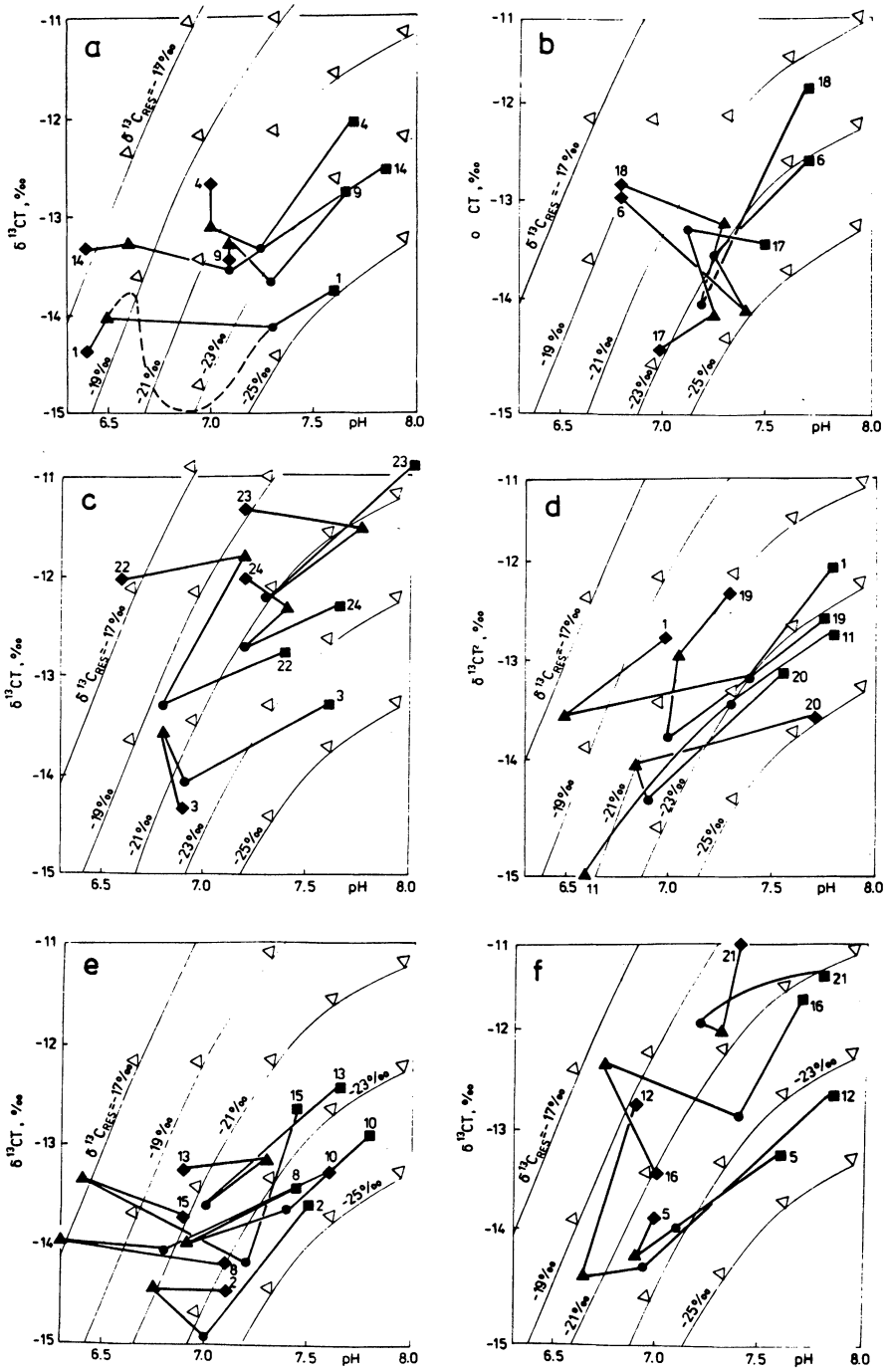

Fig. 8. Seasonal variations in $\delta^{13}CT$ and pH along the evolution lines of CSC according to Deines *et al.* (1974) ◆-January 26, 31 ▲-March 3, 16 ●-April 1 ■-May 5. The dashed line is explained in the text.

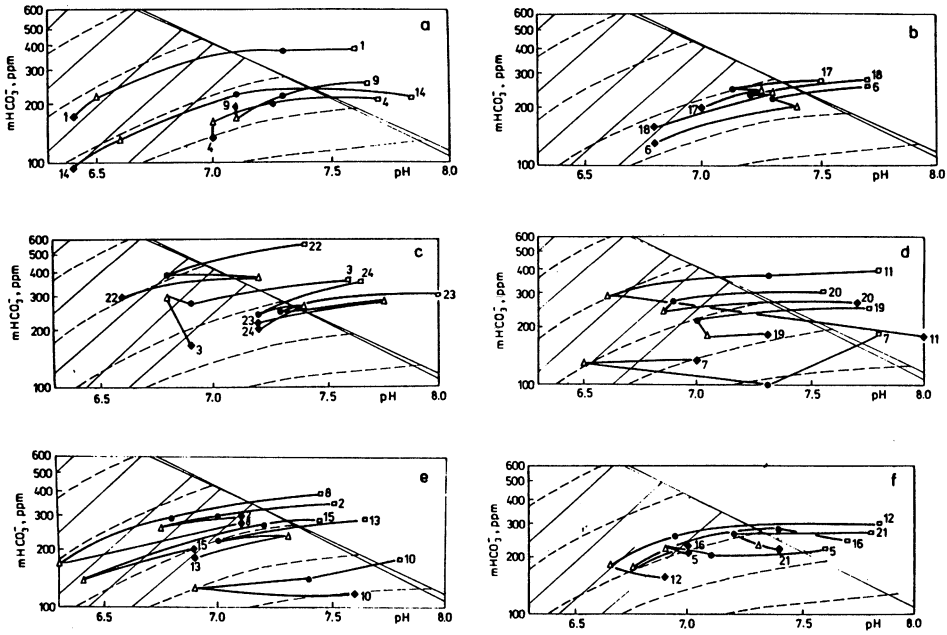

Fig. 9. Seasonal variations in $m\mathrm{HCO}_3^-$ and pH along the evolution lines of CSC. ◆-January 26, 31 △-March 3, 16 ●-April 1 □-May 5.

water. Such a loss should rather be excluded, however, because it must yield a higher slope of the curves in Figs. 8 during April. The loss of CO_2 yields higher $\delta^{13}CT$ values (Wigley *et al.* 1978).

The change in pressure of CO_2 was fast for the period of March and slow for April. A higher content CO_2 in water in February is inconsistent with the classical investigations of soil CO_2 (c.f. Russel 1978). However, these investigations concerned the gas phase of CO_2 in the soil air only. In winter majority of the soil-generated CO_2 is sorbed in the soil (Turlyun 1958). The CO_2 sorbed or in gas phase may be dissolved by water. In February the waters penetrating the soil have lower temperature than in March, so a higher content of CO_2 in water in February may be explained by higher solubility of CO_2 in cooler water as well.

From January to March histograms for $\delta^{13}C_{RES}$ indicate that water in springs and wells shows a wide range of delta values (from -17 to -27‰). This range may be a result of small, frequent, irregular inflows during autumn and winter and nonlinear effects of mixing of these waters with the aquifer water. As it has been already described above the nonlinear mixing effects may result in a significant change of water parameters even if the inflow into aquifer is small and discrete (Figs. 4, 5).

The first major inflow event in February was a result of melting of the snow and heavy rains in the second decade of the month (see Fig. 6). This inflow resulted in only a small change of the histogram profile, but in April and May $\delta^{13}C_{RES}$ values

focused in a narrow range from −22 to −26 permil. This indicates that waters in March and April evolved under lower value of $\delta^{13}C_{RES}$. These inflows significantly contributed to the amount of water accumulated in the aquifer. The reason for the decrease of $\delta^{13}C_{RES}$ is probably the development of the biological activity in late spring.

On the basis of Figs. 8 and 9 the individual changes of the parameters may be considered. Waters collected in January were, in most cases, highly undersaturated. The main feature of the curves presented in Figs. 8 and 9 is a strong variation in the chemistry and $\delta^{13}CT$ values during a period from January to April and an almost common trend in one direction since April to May. The evolution lines calculated according to Deines *et al.* (1974) nearly approximate this trend. The variations observed reflect the mixing processes which in natural waters is accompanied by carbonate dissolution. The mixing of two saturated waters yields always an undersaturated one, if only these waters differ sufficiently in PCO_2. Therefore, when the admixed water has an evolution path almost identical to the accumulated one, the chemistry of the mixture will not change at all. However, the $\delta^{13}CT$ value may be affected during mixing due to the variations in $^{13}C/^{12}C$ of carbon dioxide generated in the soil at different periods. Such situations are likely to take place in case of springs No. 1 and 14. Points in Fig. 9a lie within experimental errors on the evolution path, so they do not indicate any mixing event. The mixing process, however, is clearly visible from $\delta^{13}CT$ and pH data in Fig. 8a. A small change in $mHCO_3^-$, $\delta^{13}CT$ and pH observed in February indicates inflows of water having similar PCO_2 and $\delta^{13}CT$ to that collected in the aquifer. These inflows apparently moderated the carbonate dissolution. In March, however, curves in Fig. 9a indicate the carbonate dissolution, whereas that in Fig. 8a, indicate an admixture of water carrying inorganic carbon from CO_2-reservoir which was significantly lower in $\delta^{13}CT$ (see Fig. 5). A presumable path of $\delta^{13}CT$ versus pH for this period is shown by a dashed line in Fig. 8a.

We may notice that similar changes have been recorded for other springs, for example Nos. 6, 13, 17, 18 in February. In many samples a significant inflow of CO_2-rich water have been recorded in both Figs. 8 and 9, for example springs Nos. 2, 8, 15 in February, or springs Nos. 6, 13, 17, 18 in March.

Spring No. 24 discharging Cretaceous aquifer and wells Nos. 22 and 23, providing water from Jurassic aquifer, show similar records of the chemical and isotopic compositions. They probably take water from a common reservoir in contrast to spring No. 21 in Jurassic aquifer.

The common trend recorded in Figs. 8 and 9 for the period of April indicates the carbonate dissolution process only. The rain water during this period was either evaporated or imbibed by plants.

In another area of Lublin Upland, near Lublin, we recorded annual variation in pH value of about 0.2 only and highly stable HCO_3^- content (Staniaszek and Halas – in preparation).

Conclusions

The study area has been found very useful to prove the models of chemical evolution of carbonate ground waters. The geological structure of this area promotes to accelerate inflows of "fresh", undersaturated water to the aquifer. Those rapid inflows may be observed as significant changes of pH, $m\mathrm{HCO}_3^-$ and $\delta^{13}CT$. Results of investigation have been interpreted by the use of Deines *et al.* (1974) models, extended to include mixing of waters. Although the mixing of carbonate waters in natural conditions is frequently a continuous process, which further complicates mathematical description, the simplified model presented here may be particularly useful in the studies of infiltration time. The most remarkable changes in pH and $m\mathrm{HCO}_3^-$ are expected when the inflowing water has a partial pressure of CO_2 higher than the water accumulated in the aquifer. Such a situation frequently occurs during spring when melting and/or rainfall waters start to feed the underground reservoirs.

In the case mixing of waters terms $\delta^{13}C_{RES}$ and PCO_{2RES} lose their primary meaning due to significant nonlinear effects. However, they may be considered as indicators of the inflows which allow a precise estimation of the springs response time.

Certain conditions in the soil, as the changes of CO_2 content and the changes of the average isotopic composition of this CO_2, may still be investigated. The models of carbonate dissolution and mixing of carbonate waters have been proved to be very useful and much more sensitive than traditional measuring of springs productivity. It has also been proved that the study of chemical composition only, may be insufficient to detect a small inflow to the aquifer. The investigations should be supplemented by observation of $\delta^{13}CT$.

Acknowledgements

Dr. B. Janiec from the Institute of Hydrology at Maria Curie Sklodowska University participated in the experimental part of this work. The work was supported by the Research Program MR.I.5.

References

Ackermann, T. H. (1958) Aussagen über die Eigendissoziation des Wassers aus Molwärmemessungen gelöster Elektrolyte, *Z. Elektrochem, vol. 62,* 411-419.

Bielecka, M. (1967) The Tertiary of the South-West part of the Lublin Upland (in Polish), Biuletyn Instytutu Geologii 206, 115-169.

Craig, H. (1957) Isotopic standards for carbon and oxygen and correction factors for mass spectrometric analysis of carbon dioxide, *Geochim. Cosmochim. Acta vol. 12,* 133-149.

Deines, P. Langmuir, D., and Harmon, R. S. (1974) Stable carbon isotope ratios and the existence of a gas phase in the evolution of carbonate ground waters, *Geochim. Cosmochim. Acta, vol. 38,* 1147-1164.

Halas, S., Lis, J., Szaran, J., Trembaczowski, A., Wolacewicz, W., and Zuk, W. (1979) The carbon and oxygen isotope composition of limestones in Lublin Upland (in Polish), *Przeglad Geologiczny, vol. 27,* 162-163.

Halas, S. (1979) Automatic inlet system with pneumatic changeover valves for isotope ratio mass spectrometer, *J. Phys. E. Sci. Instrum., vol. 12,* 418-420.

Halas, S., and Skorzynski, Z. (1980) An inexpensive device for digital measurements of isotopic ratios, *J. Phys. E. Sci. Instrum., vol. 13,* 346-349.

Halas, S. and Skorzynski, Z. (1981) Economical method of on-line data processing for an isotope-ratio mass spectrometer, *J. Phys. E. Sci. Instrum., vol. 14,* 509-512.

Halas, S., Janiec, B., and Staniaszek, P. (1982) The investigation of variation of reasons of $^{13}C/^{12}C$, pH and concentration of inorganic carbon in underground waters (in Russian), IX International Symposium Stable Isotopes in Geochemistry, Moscow, 16-19 November, 447-449.

Halas, S., Janiec, B., and Staniaszek, P. (1983) Seasonal variations in chemistry and $^{13}C/^{12}C$ ratios of carbonate dissolving water, International Symposium on Isotope Hydrology in Water Resources Development, Vienna, 12/16 September. The book of extended synopses, 174.

Holland, H. D., Kirssipu, T. V., Huebner, J. S., and Oxburg, U. M. (1964) On some aspects of the chemical evolution of cave waters, *J. Geol., vol. 72,* 36-67.

Janiec, B. (1973) The preliminary results of investigation underground waters of the S-W Margin Lublin Upland and West slope of Roztocze (in Polish), Fol. Scient. Lubl., 15 Geogr. 1, 53-56.

Janiec, B. (1980) Underground waters of the S-W Margin Lublin Upland (in Polish), Ph. D. Theses, Institute of Hydrography, MCS University, Lublin.

Langmuir, D. (1971) The geochemistry of some carbonate ground waters in Central Pennsylvania, *Geochim. Cosmochim. Acta, vol. 35,* 1023-1045.

McCrea, J. M. (1950) On the isotope chemistry of carbonates and paleotemperature scale, *J. Chem. Physics., vol. 18,* 849-857.

Plummer, L. N. (1977) Defining reactions and mass transfer in part of the Floridan Aquifer, *Water Resources Research, vol. 13,* 801-812.

Plummer, L. N., Parkhurst, D. L., and Kosiur, D. R. (1975) MIX2: A computer program for modeling chemical reactions in natural waters, U.S. Geol. Survey, Water Resources Inv. 75-61, 68 pp U.S. Dept. Commerce, NTIS, Springfield, VA 22161, Accesion No. PB-251668.

Plummer, L. N., Jones, B. F., and Truesdell, A. F. (1976) WATEQF – A FORTRAN IV version of WATEQ, a computer program for calculating chemical equilibria of natural waters, U.S. Geol. Survey, Water Resources Inv., 76-13, 61 pp., NTIS Tech. Rept. PB-26-1027, Springfield, VA 22161.

Plummer, L. N., and Back, W. (1980) The mass balance approach Application to interpreting the chemical evolution of hydrologic systems, *Amer. J. Sci., vol. 280,* 130-142.

Plummer, L. N., and Busenberg, E. (1982) The solubilities of calcite, aragonite and vaterite in CO_2-H_2O solutions between 0 and 90°C, and an evaluation of the aqueous model for the system $CaCO_3$-CO_2-H_2O, *Geochim. Cosmochim. Acta, vol. 46,* 1011-1040.

Pozarycki, W. (1956) The regional geology of Poland, Region of Lublin, Cretaceous, Vol. 2, Cracow (in Polish), 14-62.

Reardon, E. J., Allison, G. B., and Fritz, P. (1979) Seasonal chemical and isotopic variations of soil CO_2 at Trout Creek, Ontario, *Journal of Hydrology, vol. 43,* 355-371.

Russell, E. W. (1973) *Soil conditions and plant growth,* 10-th ed., London, Longmans 8° s. XVIII, 849.

Staniaszek, P., and Halas, S., Chemistry and $\delta^{13}C$*T* of selected springs around Lublin City, Weakly observations from October 1982 to June 1983. (in preparation).

Staniaszek, P., and Halas, S. (1985) Simplified theory of the mixing effects of carbonate dissolving waters on chemical $^{13}C/^{12}C$ compositions, *Isotopenpraxis, vol. 21*, 12, p 424-429.

Szaran, J., and Zuk, W. (1980) Experimental investigation of kinetics and equilibrium of carbon isotopic exchange reaction in the system HCO_3^--CO_2, ZFI-Mitteilungen, 29, 48-56.

Thrailkill, J. V. (1968) Chemical and hydrologic factors in the excavation of limestones caves, *Bull. Geol. Soc. Amer., Vol. 79,* 19-4.

Truesdell, A. F., and Jones, B. F. (1974) WATEQ: A computer program for calculating chemical equilibria of natural waters, U.S. Geol. Survey J. Research 2, 233-248.

Turlyun, I. A. (1958) On the nature of the gas and vapors migration process in soils and subsoils, (in Russian) *Pocvovedenia, vol. 9,* 89-100.

Uziak, S., Klimowicz, Z., and Melke, J. (1980/1981) Some properties of soils in the part of Lublin Coal Basin with regard to lithology and organic substance contents, (in Polish) Annales UMCS sec. B v., XXXV/XXXVI 14, 227-239.

Wigley, T. M. L., and Plummer, L. N. (1976) Mixing of carbonate waters, *Geochim. Cosmochim. Acta, vol. 40,* 989-995.

Wigley, T. M. L., Plummer, L. N., and Pearson, F. J. Jr. (1978) Mass transfer and carbon isotope evolution in natural water systems, *Geochim. Cosmochim. Acta, vol. 42,* 1117-1139.

Wigley, T. M. L., Plummer, L. N., and Pearson, F. J. Jr. (1979) Errata, *Geochim. Cosmochim. Acta, vol. 43,* 13995.

Wilgat, T. (1958) Hydrographical problems of the Lublin Upland (in Polish), Czas. Geogr. v. XXIX, z. 4, Wroclaw, 497-508.

Wilgat, T. (1968) The extended hydrographic map of Lublin Region. (in Polish), Annales UMCS sec. B, v. XX, z. 10, Lublin, 223-242.

First received: 22 February, 1985
Revised version received: 5 December, 1985

Address:
S. Halas,
Institute of Physics,
Maria Curie- Sklodowska University,
20-031 Lublin,
Poland.

P. Staniaszek,
Department of Physics,
Memorial University of Newfoundland,
St. John's, Newfoundland,
Canada A1B 3X7.